# Novel Method to Assess Motion Blur Kernel Parameters and Comparative Study of Restoration Techniques Using Different Image Layouts

by

Munira Akter Lata (Roll: 120061)
Supriti Ghosh (Roll:120098)
Farjana Bobi (Roll:120054)

A Thesis Report submitted to the Institute of Information Technology
in partial fulfillment of the requirements for the degree of
Bachelor of Science

Supervisor: Dr.Mohammad Abu Yousuf

Institute of Information Technology
Jahangirnagar University
Savar, Dhaka-1342
January 25, 2016

# DECLARATION

We hereby declare that this thesis is based on the results found by ourselves. Materials of work found by other researcher are mentioned by reference. This thesis, neither in whole nor in part, has been previously submitted for any degree.

| | | |
|---|---|---|
| Munira Akter Lata | Supriti Ghosh | Farjana Bobi |
| Roll:120061 | Roll:120098 | Roll:120054 |

# CERTIFICATE

This is to certify that the thesis entitled **Novel Method to Assess Motion Blur Kernel Parameters and Comparative Study of Restoration Techniques Using Different Image Layouts** has been prepared and submitted by **Munira Aktar Lata**, **Supriti Ghosh** and **Farjana Bobi** in partial fulfillment of the requirement for the degree of Bachelor of Science (honors) in Information Technology on January 25, 2016.

Mohammad Abu Yousuf
Supervisor

Accepted and approved in partial fulfilment of the requirement for the degree Bachelor of Science (honors) in Information Technology.

| | |
|---|---|
| Mohammad Abu Yousuf<br>Chairman | Mrs Risala Tasin khan<br>Member |
| Md. Zamshed Iqbal Chowdhury<br>Member | Prof. Dr. M. A. Mottalib<br>Member (External) |

# ACKNOWLEDGEMENTS

We feel pleased to have the opportunity of expressing our heartfelt thanks and gratitude to those who all rendered their cooperation in making this report.

This thesis is performed under the supervision of Dr.Mohammad Abu Yousuf, Assistant professor, Institute of Information Technology (IIT), Jahangirnagar University, Savar, Dhaka. During the work, he has supplied us a number of books, journals, and materials related to the present investigation. Without his help, kind support and generous time spans he has given, we could not perform the project work successfully in due time. First and foremost, we wish to acknowledge our profound and sincere gratitude to him for his guidance, valuable suggestions, encouragement and cordial cooperation.

We express our utmost gratitude to K M Akkas Ali, Director, IIT, Jahangirnagar University, Savar, Dhaka, for his valuable advices that have encouraged us to complete the work within the time frame. Moreover, we would also like to thank the other faculty members of IIT who have helped us directly or indirectly by providing their valuable support in completing this work.

We express our gratitude to all other sources from where we have found help. We are indebted to those who have helped us directly or indirectly in completing this work.

Last but not least, we would like to thank all the staff of IIT, Jahangirnagar University and our friends who have helped us by giving their encouragement and cooperation throughout the work.

# ABSTRACT

In general, images are yielded to preserve or represent convenient information. The recorded image can perpetually characterizes a degraded version of the original image caused by inadequacy in the imaging and capturing process. There exists several kinds of degradations that need to be considered to restore degraded images. Such kinds of degradations are blur, illumination and color imperfections, geometrical degradations and noise. Among those, two major categories of degradations namely, motion blur and noise are considered in this study. Motion blur occurs when there is movement of element or camera or both during exposure time. Besides to this blurring effect, noise also debase any recorded image. Therefore, restoration of motion blur image and reduction of noise are very important in many circumstances like identification of criminals and tracking vehicles number plate. For restoring degraded image, it is important to know the degradation function, commonly point spread function (PSF) of blurred image. The point spread function is defined by two parameters called, blur direction and blur length. This study focuses an approach to assess the parameters from blurred and noisy images. Furthermore, this study presents comparative analysis of different non-blind image restoration techniques based on Wiener and Lucy-Richardson algorithm for different types of image layouts such as .tif (Tag Index Format), .jpg (Joint Photographic Experts Group) and .png (Portable Network Graphics). The experimental result illustrates blur images without noise and with noise are successfully restored.

# TABLE OF CONTENTS

# LIST OF FIGURES

**Figure**

# LIST OF TABLES

**Table**

# LIST OF NOTATIONS

| | |
|---|---|
| $o(x, y)$ | Experimental Image |
| $d(x, y)$ | Degradation Function |
| $f(x, y)$ | Original Image |
| $n(x, y)$ | Additive Noise |
| $(k, l)$ | Spatial Frequency Coordinates |
| $O, F, DandN$ | Fourier Transforms |
| $\alpha$ | Blur Angle |
| $V$ | Constant Relative Velocity |
| $E$ | Blur Length |
| $T$ | Disclosure Time |
| $D(k)$ | Verticle Frequency Coordinate |
| $A \star B$ | Image Size |
| $C$ | Width of the Window Function |
| $\alpha_{min}$ | Lowest Value of Blur Angle |
| $\alpha_{max}$ | Highest Value of Blur Angle |
| $(x, y)$ | Cartesian Coordinate |
| $(x_i, y_i)$ | Edge Point |
| $M_f(l, k)$ | Power Spectrum of Original Image |

| | |
|---|---|
| $M_n(l,k)$ | Power Spectrum of Noise Image |
| $k$ | Constant and Experiment Reveal |
| $w$ | Image Width |
| $d_{ir}$ | Point Spread Function |
| $i$ | Position of Pixel Value |
| $a_r$ | Blurred Image Pixel Value at Position i |

l

# LIST OF ABBREVIATIONS

| | |
|---|---|
| **PSF** | Point Spread Function |
| **MSE** | Mean Square Error |
| **RMSE** | Root Mean Square Error |
| **NMAE** | Normalized Mean Absolute Error |
| **PSNR** | Peak Signal to Noise Ratio |
| **.tif** | Tag Index Format |
| **.jpg** | Joint Photographic Experts Group |
| **.png** | Portable Networ Graphics |

# CHAPTER I

# Introduction

## 1.1 Overview

Motion blur is an undesired effect on an image due to camera shake during exposure, a long aperture time, atmospheric turbulence, wrong focusing of lens, relative motion between photographic device and original scene. In image processing system, it is important to regain the original image from a degraded image which is blurred by a degradation function.

This study represent an improved frequency based method to find out motion blur PSF parameters and our contribution lies in five aspects:

- A simple preprocessing step called Hann windowing is pretended for anti-artifacts to improve restored image quality.
- Hough transform is adopted for accurate estimation of the blur direction efficiently. To find the blur length, the binarized spectrum of the blurred image is rotated in the estimated direction and convert the 2-D spectrum into 1-D spectrum. After that the first negative value is determined that corresponds to blur length.
- Wiener filter based approach and Lucy-Richardson algorithm are used to restore different types of images after getting the approximated parameters.

- Measure the qualitative performance of Wiener filter and Lucy-Richardson based on several performance metrics like Mean Square Error (MSE), Root Mean Square Error (RMSE), Normalized Mean Absolute Error (NMAE) and Peak Signal to Noise Ratio (PSNR).

- Finally, evaluate which restoration technique is suitable for which kind of image layout namely, .tif(Tag Index Format),.jpg(Joint Photographic Experts Group),.png(Portable Network Graphics).

Figure1.1 represents the steps of restoring the blurred image which we have proposed in this paper.

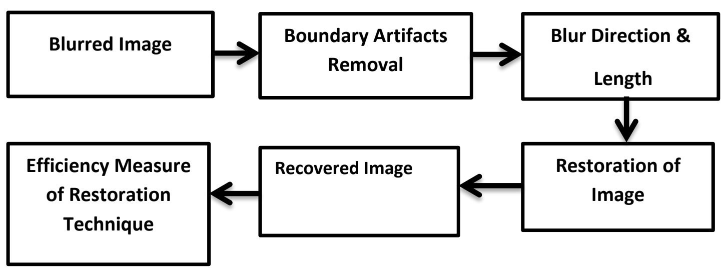


Figure 1.1: Procedure of the proposed system

## 1.2 Problem Statement

Image restoration is an objective process which attempts is to recover an image that has been degraded. Without previous knowledge of the degradation phenomenon it is not possible to restore an image. Hence it is required to estimate the degradation function. Many types of degradations can be approximated by linear, position invariant processes. In our study we work with degradation function that is previously known to us.

## 1.3 Objectives

The principle objective of our study is to restore a degraded image in some predefined sense. We work by consideration of some objectives that are stated below:

- The principle objective of our study is to reconstruct motion blurred image.
- To improve restored image quality by removing boundary artifacts.
- To apply non-blind restoration techniques for several image layouts such as .tif, .jpg and .png.
- To determine which restoration technique is suitable for which kind of image.
- To use various performance matrics like Mean Square Error (MSE), Root Mean Square Error (RMSE), Normalized Mean Absolute Error (NMAE) and Peak Signal to Noise Ratio (PSNR) for determining the efficiency of restoration techniques.

## 1.4 Assumptions and Limitations

Our proposed method is not work directly with color images, at first we need to convert images in gray scale. Which limits our work. In case of restoration technique called Wiener filter we need to know power spectrum of the undegraded image and noise. But it is not possible to know the power spectrum of the undegraded image, hence, we estimate the ratio between power spectrum of noise and undegraded image through assumption.

## 1.5 Comprehensive Analysis with Existing Study

[20] This study considered only wiener based method to restore degraded image. Theres no idea about improvement of image quality. [21] This study considered only one single photograph. No approximation about another type of image layouts. [1] This study about removal of Gaussian noise. No focusing about impulse noise that is frequent during image acquisition.

In our study

1.we represents two non-blind image restoration techniques based on Wiener method and Lucy-Richardson method. An image quality increasing method called Hann window also adopted.

2.Three different image layouts are considered and detect which restoration technique suitable for which image layout.

3.Impulse noise taken into account which is more frequent than Gaussian noise due to faulty sensor.

## 1.6 Thesis Outline

This study is arranged as section II contains related works. The degradation model of images is described in section III. Section IV represents the preprocessing step namely Hann windowing to improve restored image quality. Algorithms to assess blur functions have been discussed in section V. Section VI represent the comparison of non-blind restoration method. Experimental results are shown in section VII. Finally, section VIII represents conclusion and discussions.

# CHAPTER II

# Literature Review

Several methods have been proposed in literatures to identify blur parameters and to restore blurred images.

A Cepstral based blind deconvolution method has proposed by Haruka Asai, Yuji Oyamada, Julien Pilet and Hideo Saito [1] and the algorithm can restore the blurred image using blinddeconvolution method.

Michal Dobes, Libor Machala, Tomas Furst has proposed a method to discover the motion angle and length for blurred image restoration and the method is based on power spectrum of the image slope in the frequency domain [2].

Shamik Tiwari, V. P, Shukla, Ajay Kr. Singh [3] compares different approaches to detect and estimate the parameters such as blur direction and blur length of a motion blur from the image.

To estimate both the length (also for small length) and knowing the motion blur kernels is represented by Joao P. A. Oliveira, Mario A. T. Figueiredo and Jose M. Bioucas-Dias [4] and they also represents that the angular invariance of natural images spectrum is abused in the Radon transform domain.

Hui Ji, Zuowei Shen and Yuhong Xu has proposed a wavelet frame based image restoration and a regularization based approach to recover degraded images by enforcing the analysis based insufficiency prior of images in tight frame domain [5].

Hongwei Sun, Michel Desvignes, Yunhui Yan, Weiwei Liu represents how to identify the parameters of motion blur from the gradient of the observed image [6].

Wikky Fawwaz A M, Takuya Shimahashi, Mitsuru Matsubara and Sueo Sugimoto [7] has proposed an idea about PSF parameters estimation and noiseless motion blurred image restoration in spatial domain.

[10] R.L.Lagendijk and J.Biemond represents basic Methods for Image Restoration and Identification.

I.Rekleitis has proposed [11] an idea about vision motion estimation based on motion blur interpretation.

M.Cannon represents blind deconvolution of spatially invariant image blurs with phase [12].

[13] J. S. Lim represents image restoration by short space spectralsubtraction.

Deepa Kundur, Dimitrios Hatzinakos [14] has proposed a novel blind deconvolution scheme for image restoration using recursive filtering.

Reginald L. Lagendijk, Jan Biemond and Dick E. Boekee has proposed identification and restoration of noisy blurred images using the expectation-maximization algorithm [15].

[16] Alex Rav-Acha, Shmuel Peleg has proposed restoration of multiple images with motion blur in different directions.

Y. Yitzhaky, I. Mor, A. Lantzman and N. S. Kopeika [17] has proposed direct method for restoration of motion-blurred images.

Andreas Savakis, H. Joel Trussel has proposed on the accuracy of PSF representation in image restoration [18].

[19] Yuying Lu and Fadil Santosa has proposed a computational algorithm for minimizing total variation in image restoration.

# CHAPTER III

# DEGRADATION MODEL OF IMAGE

The degradation model of image can be shown in Figure 3.1:

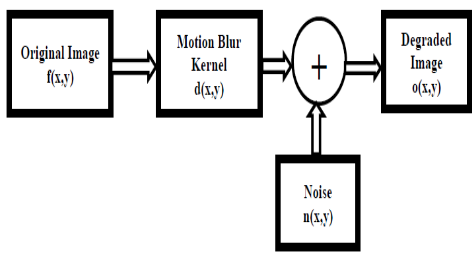


Figure 3.1: Degradation model of images

The mathematical representation of the degradation model [8] is shown below:

$$o(x, y) = d(x, y) \star f(x, y) + n(x, y) = \sum_{i=0}^{A-1} \sum_{j=0}^{B-1} d(x - i, y - j) f(x, y) + n(x, y) \quad (3.1)$$

where o(x,y) is the experimental image, degradation function is d(x,y),f(x,y)is the original image, and the additive noise is n(x,y) which is Gaussian white noise with zero mean. The convolution operator is (*) and size of all images represented by A*B, where A and B express the image size in x and y axis respectively. Eq. 3.1 in frequency domain can be written as follows,

$$o(k,l) = F(k,l)D(k,l) + N(k,l) \tag{3.2}$$

Because, convolution in spatial domain is equal to multiplication in frequency domain. Where spatial frequency coordinates are (k,l) and O,F,D and N represent the Fourier transforms of the experimental image o,original image f, degradation function d and noise n respectively. If we consider the point spread function d(x,y) is undeviating and space invariant function, then the noisy or blurred image is in spatial domain and it can be represented as,

$$d(x,y) = \{^{\frac{1}{E}, if 0 \leq x \leq E \cos\alpha; y = E \sin\alpha}_{0, otherwise} \tag{3.3}$$

This paper contains images blurred by the uniform linear motion between the sensor and the image during image possession. When the scene to be recorded at constant relative velocity V between the photographic device and the scene with an angle $\alpha$ degrees laterally the horizontal axis during the disclosure time [0, T], then the motion blur PSF d(x,y) for blur length E=VT [10,11] is given in Eq. 3.3.
To avoid the complexity, we assume that motion is laterally the horizontal direction i.e $\alpha = 0$, then Eq. 3.3 can be derived as,

$$d(x,y) = \{^{\frac{1}{E}, if 0 \leq x \leq E \cos\alpha; y = 0}_{0, otherwise} \tag{3.4}$$

Deal with

$$\sin x = \{frac12j[e^{jx} - e^{-jx}]$$

on the Fourier transform of Eq. 3.4,we get,

$$D(k) = \sin c(\Pi k E) e^{-j\Pi k E} \tag{3.5}$$

The magnitude transfer function of Eq. 3.5 can be shown as,

$$|D(k)| = \sin c(\Pi k E) \tag{3.6}$$

Mark that D(k) is autonomous of the vertical frequency coordinate l. In the same manner, the expression for motion blur point spread function of blur length E whose blur angle $\alpha^2$ with the horizontal axis is found in [12] and given by,

$$D(k,l) = \sin(\Pi E f); where f = k \cos\alpha + l \sin\alpha \tag{3.7}$$

# CHAPTER IV

# BOUNDARY ARTIFACTS REMOVAL

To improve the quality of restored image, boundary artifacts removal is necessary. Practically, real image has limited in its size but the Fourier transform treats image data as being infinite. Consequently, an infinite periodic signal is obtained by Fourier transform. Thus, it is essential to change the real signal with a windowing function to remove the hasty changes along the borders. In digital image processing system, several windowing functions like Blackman, Kaiser, Hann, Gaussian, Tukey, Lanczos, Hamming windows are available. This study represents Hann windowing because of its truncated aliasing. The coefficients of a Hann window are computes as Eq.4.1 .

$$w(n) = 0.5(1 - \cos(\{frac2\Pi nc - 1)) \tag{4.1}$$

where

$$n\epsilon 0, 1, , , , , , C - 1$$

with C being the width of the window function.

# CHAPTER V

# ASSESSMENT OF BLUR FUNCTIONS

Line of action to find blur direction [10] and cepstral method to find blur length [1] are discussed in this section.

## 5.1 Assessment of Blur Direction

We can identify the blur direction by observing that the non-blurred original images spectrum is isotropic and the spectrum of blurred image is anisotropic. A motion blurred image is usually expressed by a linear system of a convolution $o(x, y) = f(x, y) \star d(x, y)$ where d(x,y) is the convolution kernel. This convolution kernel is responsible for occurring the motion blur. The anisotropy in the spectrum bring forward by the motion blur is in the orientation, always perpendicular to the direction of the motion. The spectrum is considered as an image for determining the blur direction. Then we use Hough transform to detect the act of turning of the line in the spectrum. Algorithm 1 represents the procedure to detect the line in the spectrum.

**ALGORITHM 1:DETECT LINE**

1. Consider, $\theta_{min}$ and $\theta_{max}$ be the lowest and highest values of $\theta$.

2. Create a 2-D array (said accumulator array) as H(r,$\theta$) and initialized with zeros.

3. for each edge point $(x_i - y_i)$compute all possible lines and increment the associated locations from H:

for each $\theta$ from 0 to $\theta_{max}$ (with a step of $\Delta\theta$)

compute $r = x_i \cos\theta + y_i \sin\theta$

increment H(r,$\theta$)

end for

4. Detect the highest value of the accumulator array as $H(p_{max}, \theta_{max})$ .

5. Hence, get the corresponding line as

$r_{max} = x\cos(\theta_{max}) + y\sin(\theta_{max})$

end

The Hough transform method is very useful for finding lines in an image that contains a set of interest point. The pre-processing of Hough transform requires the edge in an image to be extracted out. By using Hough transform it is easy to detect the lines as points, based on the polar representation of line:

$$r = x\cos\theta + y\sin\theta \tag{5.1}$$

where (x,y) corresponds to Cartesian coordinates of a point on the line, $\theta$ is the angle between the origin to the given line and the x-axis and p is the perpendicular length. So the line can be described as a pair of coordinates $(r, \theta)$ The parameter space into accumulator cells is divided by the Hough transform. It returns the peak

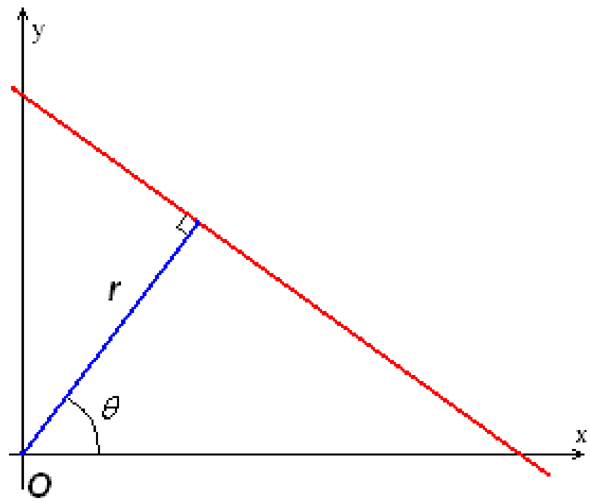


Figure 5.1: $(r, \theta)$ parameterization of line in the xy-plane

value of the accumulator array.Figure 5.1 illustrates the geometrical interpretation of the parameters r and $\theta$. A horizontal line $\theta = 0^o$, with $\rho$ being equal to the position x-intercept.Similarly , a vertical line has $\theta = 90^o$, with $\rho$ being equal to the positive y-intercept, or $\theta = -90^o$, with $\rho$ being equal to the negetive y-intercept.

By locating the peak value of this accumulator we find the blur direction. To condense the computation cost of the Hough transform, the binarized spectrum is considered. Algorithm 2 represents the procedure to detect the blur direction.

**ALGORITHM 2:DETECT BLUR DIRECTION**

1. Transform the blurred RGB image into gray level image.
2. Remove the boundary artifacts of the image by performing Hann window.
3. Determine the Fourier transform O(k,l) of step 2 image.
4. Compute the log spectrum of O(k,l).
5. Calculate the Inverse Fourier transform (IFT) of log spectrum.
6. Detect the edge map of the Cepstral of step 5.
7. Derived the accumulator array by using Hough transform.
8. Find the peak in Hough transform which corresponds to blur direction.

end

## 5.2 Assessment of Blur Length

The Fourier transform of experimental image is same as the multiplication of Fourier transform of PSF and original image, when noise is ignored. The frequency rejoinder of the motion blur PSF is denoted by Eq. 3.3 and its magnitude is given by Eq. 3.6, which considered by episodic zeros on the k-axis and occur at

$$K = \pm\frac{1}{E}, \pm\frac{2}{E}, \pm\frac{3}{E}, ..... \tag{5.2}$$

We can detect the blur length by observing the zero in O(k,l). Because, zero crossing would occur periodically in D(k,l) or equivalently in O(k,l) along the lines perpendicular to the motion direction.

The process for detecting blur length is given in Algorithm 3. The algorithm is proposed with consideration of no noise. In the presence of noise, similar algorithm is applied with the difference that the blurred image is mean filtered before calculating its Fourier transform. Assume that white Gaussian noise with zero mean hence, mean filter effectively remove the Gaussian noise.

**ALGORITHM 3: DETECT BLUR LENGTH**

1. Transform the blurred RGB image into gray level image.
2. Remove the boundary artifacts of the image by performing Hann window.
3. Determine the Fourier transform O(k,l) of step 2 image.
4. Compute the log spectrum of O(k,l) and transform it in binary.
5. Binary spectrum is rotated in the direction opposite to the blur orientation.
6. Taking average along the columns to collapse the 2-D data into 1-D data.
7. Calculate the Inverse Fourier transform of 1-D data in step 6.
8. Detect the blur length using the real part of first negative value.

end

# CHAPTER VI

# BLURRED IMAGE RECONSTRUCTION WITH DIFFERENT RESTORATION METHODS

Non-blind image restoration techniques are used to restructure degraded images in the presence of acknowledged PSF. In this section comparison of two non-blind techniques viz. Wiener filter and Lucy-Richardson method are discussed.

## 6.1 Restoration Technique Based on Wiener Method

In restoration method, Wiener filter [8] treats images and noise as random variables. The purpose of Wiener filter is to detect an estimate $\hat{f}$ of the original image f means that the mean square error between them is minimized. Its transfer function [8] is given by:

$$\hat{F}(k,l) = [\frac{D\star(k,l)M_f(k,l)}{M_f(k,l)|D()k,l|^2 + M_n(k,l)}]O(k,l) \tag{6.1}$$

where D(k,l) is the frequency response of PSF d(x,y),$D\star(k,l)$ the complex conjugate of D(k,l),$|D(k,l)|^2 = D\star(k,l)D(k,l)$ and the power spectrum of original image and noise are $M_f(k,l)$ and $M_n(k,l)$ respectively.

Inverse Fourier transform transfer the restored image in spatial domain. Wiener filter is reduced in Inverse filter due to the vanishing of noise power spectrum when noise is zero [13]. The information of the power spectrum of the original image is required by Eq. 5.1 which is hardly known. Then the Eq. 5.1 can be approximated by the following expression

$$\hat{F}(k,l) = [\frac{D \star (k,l)}{|D(k,l)|^2 + K}]O(K,l) \tag{6.2}$$

where K is constant which can be determined through experiments. A good estimate for the value of $K$ is $\frac{1}{w}$ . Here, w is the images width. The details method of motion blurred image restoration is given in Algorithm 4. In this paper, different image quality measures have been calculated like MSE, RMSE, NMAE and PSSNR to assess the efficiency of FFT technique.

a1.) MSE: MSE is defined as the some sort of average or sum of square of the error between original image and restored image. This is given by the statistical form as follows,

$$MSE = \frac{1}{AB} \sum_{x=0}^{A-1} \sum_{y=0}^{B-1} [f(x,y) - \hat{f}(x,y)]^2 \tag{6.3}$$

where f(x,y) and $\hat{f}(x,y)$ are real and restored image respectively and A, B is the dimensions of both image. Hence, lower value of this measure expose better restoration.

a2.) RMSE : RMSE is stated as the square root of mean square error. Thus, RMSE = MSE.

a3.)NMAE: NMAE is considered to find the similarities between images, which is Hamming Distance between images computing the average number of different pixel values. Hence, lower value of this measure expose better restoration.

a4.) PSNR: PSNR is defined as ratio of power of original image to the power of corrupting noise. Bigger value of this measure signifies better restoration.

This is given by the statistical form as follows,

$$PSNR = \sum_{x=0}^{A-1} \sum_{y=0}^{B-1} [\hat{f}(x,y)]^2 / \sum_{x=0}^{A-1} \sum_{y=0}^{B-1} [f(x,y) - \hat{f}(x,y)]^2 \tag{6.4}$$

**ALGORITHM 4: RESTORATION of BLUR IMAGE**

1. Use the algorithm DETECT BLUR DIRECTION to identify the blur direction.

2. Use the algorithm DETECT BLUR LENGTH to identify the blur length.

3. Use the blur direction and blur length to form the PSF.

4. Convert PSF to optical transfer function (OTF) of desired size.

5. Compute the spectrum of Wiener filter as follows:

$$W(k,l) = [\frac{D \star (k,l)}{|D(k,l)|^2 + K}]$$

6. Compute the multiplication between Fourier transform of blurred image O(k,l) and Wiener filter to get the Fourier transform $\hat{F}(k,l)$ of the original image.

7. Take the Inverse Fourier transform of $\hat{F}(k,l)$ to obtained the restored image.

end

## 6.2 Restoration Technique Based on Lucy-Richardson Method

Lucy-Richardson based technique is another type of non-blind image restoration technique which possess iterative procedure. This algorithm maximizes probability of restored image when convolved with PSF. If $h_i$ is the observed value at pixel position i then, it can be given as Eq. 6.5.

$$h_i = \sum d_{ir} a_r \tag{6.5}$$

Where, $d_{ir}$ is the PSF, the segment of light coming from true position r that is observed at position i, $a_r$ is the blurred image pixel value at position i. Mathematical representation of the iterative process to calculate $a_r$ is given as Eq. 6.6

$$a_r^{(t+1)} = a_r^{(t)} \sum \frac{h_i}{b_i} d_{ir} \tag{6.6}$$

Where $d_{ir}$ is PSF $b_i = \sum d_{ir} a_r^{(t)}$

**ALGORITHM 5: Lucy-Richardson Algorithm**

1. Read Image
2. Simulate a Blur and Noise
3. Restore the Blurred and Noisy Image
4. Iterate to Explore the Restoration
5. Control Noise Amplification by Damping
6. Create Sample Image
7. Simulate a Blur
8. Provide the WEIGHT Array
9. Provide a finer-sampled PSF

end.

Use the deconvlucy function to deblur an image using the accelerated, damped, Lucy-Richardson algorithm. The algorithm maximizes the likelihood that the resulting image, when convolved with the PSF, is an instance of the blurred image, assuming Poisson noise statistics.

This function can be effective when we know the PSF but know little about the additive noise in the image.

**Reducing the Effect of Noise Amplification:**Noise amplification is a common problem of maximum likelihood methods that attempt to fit data as closely as possible. After many iterations, the restored image can have a speckled appearance, especially for a smooth object observed at low signal-to-noise ratios. These speckles do not represent any real structure in the image, but are artifacts of fitting the noise in the image too closely.

To control noise amplification, the deconvlucy function uses a damping parameter, DAMPAR. This parameter specifies the threshold level for the deviation of the resulting image from the original image, below which damping occurs. For pixels that deviate in the vicinity of their original values, iterations are suppressed.

Damping is also used to reduce ringing, the appearance of high-frequency structures in a restored image. Ringing is not necessarily the result of noise amplification. See Avoiding Ringing in Deblurred Images for more information.

The deconvlucy function implements several adaptations to the original Lucy-Richardson maximum likelihood algorithm that address complex image restoration tasks.

**Accounting for Nonuniform Image Quality:**Another complication of real-life image restoration is that the data might include bad pixels, or that the quality of the receiving pixels might vary with time and position. By specifying the WEIGHT array parameter with the deconvlucy function, we can specify that certain pixels in the image be ignored. To ignore a pixel, assign a weight of zero to the element in the

WEIGHT array that corresponds to the pixel in the image.

The algorithm converges on predicted values for the bad pixels based on the information from neighborhood pixels. The variation in the detector response from pixel to pixel (the so-called flat-field correction) can also be accommodated by the WEIGHT array. Instead of assigning a weight of 1.0 to the good pixels, we can specify fractional values and weight the pixels according to the amount of the flat-field correction.

Handling Camera Read-Out Noise:Noise in charge coupled device (CCD) detectors has two primary components:

- Photon counting noise with a Poisson distribution.

- Read-out noise with a Gaussian distribution.

The Lucy-Richardson iterations intrinsically account for the first type of noise. we must account for the second type of noise; otherwise, it can cause pixels with low levels of incident photons to have negative values.

The deconvlucy function uses the READOUT input parameter to handle camera read-out noise. The value of this parameter is typically the sum of the read-out noise variance and the background noise (e.g., number of counts from the background radiation). The value of the READOUT parameter specifies an offset that ensures that all values are positive.

**Handling Undersampled Images:**The restoration of undersampled data can be improved significantly if it is done on a finer grid. The deconvlucy function uses the SUBSMPL parameter to specify the subsampling rate, if the PSF is known to have a higher resolution.

If the undersampled data is the result of camera pixel binning during image acquisition, the PSF observed at each pixel rate can serve as a finer grid PSF. Otherwise, the PSF can be obtained via observations taken at subpixel offsets or via optical modeling techniques. This method is especially effective for images of stars (high signal-to-noise ratio), because the stars are effectively forced to be in the center of a pixel. If a star is centered between pixels, it is restored as a combination of the neighboring pixels. A finer grid redirects the consequent spreading of the star flux back to the center of the star's image.

**Refining the Result:**The deconvlucy function, by default, performs multiple iterations of the deblurring process. we can stop the processing after a certain number of iterations to check the result, and then restart the iterations from the point where processing stopped. To do this, pass in the input image as a cell array, for example, BlurredNoisy. The deconvlucy function returns the output image as a cell array that we can then pass as an input argument to deconvlucy to restart the deconvolution.

# CHAPTER VII

# EXPERIMENTAL RESULTS

The experiments are carried out on gray level images with both artificial motion blur and noise. Artificial blurring is done using dissimilar values of blur direction and blur length.

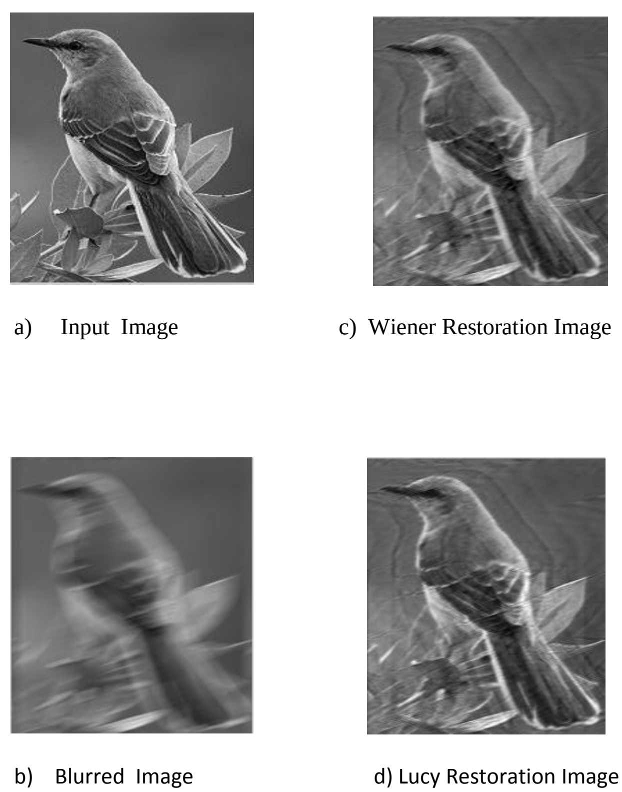


Figure 7.1: Restoration result for Bird.tif with blur direction $20^o$ and length 19.


a) Input Image c) Wiener Restoration Image

b) Blurred Image d) Lucy Restoration Image

Figure 7.2: Restoration result for Quote.jpg with blur direction $10^o$ and length 11.

Figure.7.1,7.2,7.3 shows restoration result of images without noise where, Bird.tif restored with blur direction $20^o$ and length 19, Quote.jpg restored with blur direction 10 and length 11, Fruits.png restored with blur direction $17^o$ and length 13 respectively.

Figure. 7.4,7,8 shows restoration result of images with noise where, Bird.tif restored with blur direction 20,length 19 and noise density 20 dB, Quote.jpg restored with blur direction $10^o$, length 11 and noise density 23 dB, Fruits.png restored with blur direction $17^o$, length 13 and noise density 24 dB respectively.

In table.7.2 column no 2 and 3 shows the blur direction and length used for blurring the images, assessed blur direction and length without noise are shows in column no 3 and 4 respectively.

In table.7.2 column no 2 shows noise density. Column no 3 and 4 shows the blur direction and length used for blurring the images, assessed blur direction and length


Figure 7.3: Restoration result for Fruits.png with blur direction $17^o$ and length 13.

Table 7.1: Detected blur direction and blur length for artificially blurred images without noise

| Image Used | Blur Direction | Blur Length | Assessed Direction | Assessed Length |
|---|---|---|---|---|
| Bird.tif | 10 | 12 | 12 | 13 |
| Bird.tif | 20 | 18 | 20 | 19 |
| Bird.tif | 55 | 37 | 54 | 37 |
| Quote.jpg | 30 | 21 | 30 | 21 |
| Quote.jpg | 22 | 11 | 19 | 11 |
| Quote.jpg | 45 | 37 | 45 | 37 |
| Fruits.png | 11 | 9 | 9 | 12 |
| Fruits.png | 17 | 13 | 16 | 14 |
| Fruits.png | 33 | 19 | 34 | 19 |

with noise are shows in column no 5 and 6 respectively.

In table.7.3, Bird.tif restored with blur direction 20 and length 19, Quote.jpg restored with blur direction 10 and length 11, Fruits.png restored with blur direction 17 and length 13 and column no 2, 3, 4 shows the performance metrics namely, MSE, RMSE, NMAE, PSNR of restored images for Wiener based and Lucy-Richardson

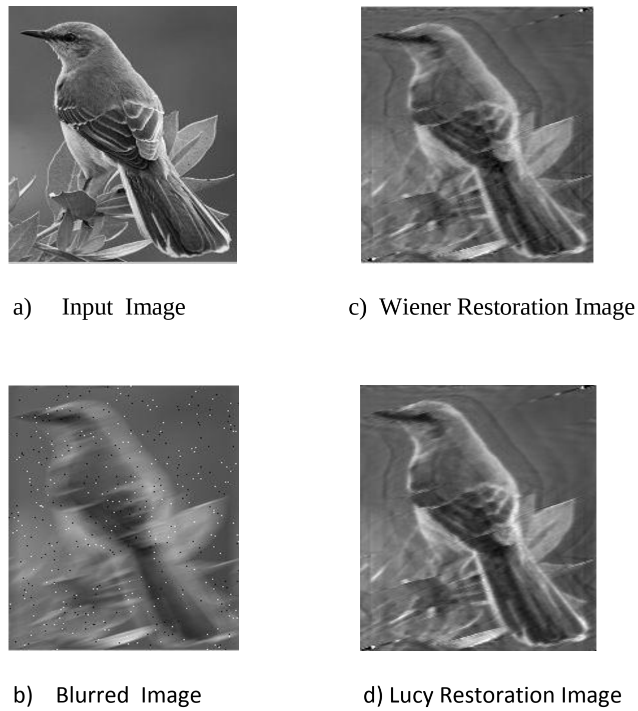


Figure 7.4: Restoration result for Bird.tif with blur direction $20^o$,length 19 and noise density 20 dB.

based technique respectively.


Figure 7.5: Restoration result for Quote.jpg with blur direction $10^o$,length 11 and noise density 23 dB

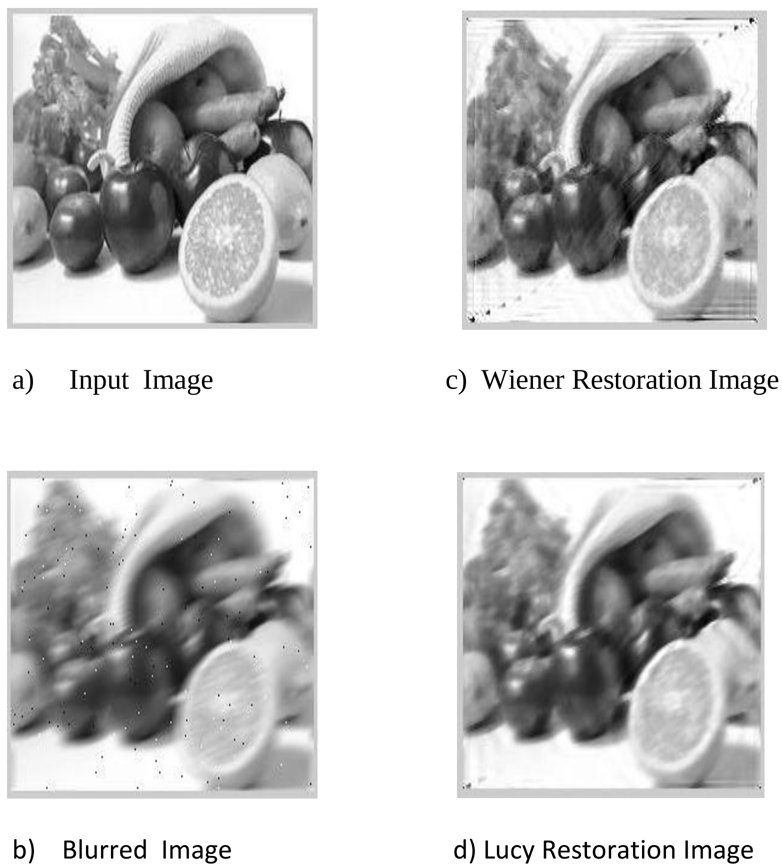

a) Input Image

c) Wiener Restoration Image

b) Blurred Image

d) Lucy Restoration Image

Figure 7.6: Restoration result for Fruits.png with blur direction $17^o$,length 13 and noise density 24 dB.

Table 7.2: Detected blur direction and blur length for artificially blurred images with noise

| Image Used | Noise Density(dB) | Blur Direction | Blur Length | Assessed Direction | Assessed Length |
|---|---|---|---|---|---|
| Bird.tif | 33 | 20 | 11 | 16 | 11 |
| Bird.tif | 31 | 50 | 17 | 55 | 18 |
| Bird.tif | 10 | 30 | 14 | 29 | 14 |
| Quote.jpg | 13 | 16 | 13 | 14 | 15 |
| Quote.jpg | 20 | 35 | 11 | 46 | 10 |
| Quote.jpg | 16 | 47 | 19 | 45 | 20 |
| Fruits.png | 23 | 15 | 18 | 16 | 18 |
| Fruits.png | 30 | 45 | 18 | 45 | 18 |
| Fruits.png | 15 | 20 | 12 | 35 | 13 |

Table 7.3: Performance measure of restoration techniques

| Image Used | Performance Metrics | Restoration Tech. Based on Wiener Method | Restoration Tech. Based on Lucy Method |
|---|---|---|---|
| Bird.tif | MSE | 0.0042 | 0.0036 |
| Bird.tif | RMSE | 0.0647 | 0.0599 |
| Bird.tif | NMAE | 0.0429 | 0.0401 |
| Bird.tif | PSNR | 23.7539 | 24.4235 |
| Quote.jpg | MSE | 0.0116 | 0.0112 |
| Quote.jpg | RMSE | 0.1079 | 0.1058 |
| Quote.jpg | NMAE | 0.0734 | 0.0803 |
| Quote.jpg | PSNR | 19.3388 | 19.5078 |
| Fruits.png | MSE | 0.0010 | 0.0011 |
| Fruits.png | RMSE | 0.0320 | 0.0328 |
| Fruits.png | NMAE | 0.0226 | 0.0234 |
| Fruits.png | PSNR | 29.9092 | 29.6722 |

## CHAPTER VIII

# Conclusion

This study presents algorithms to estimate the blur kernel parameters namely, blur direction and blur length from degraded image. Hann windowing technique has been proposed in this study to reduce the boundary artifacts of the restored image. Wiener based and Lucy-Richardson based technique are used to restore both motion blurred and noisy images. Several performance metrics such as MSE, RMSE, NMAE, PSNR are used to evaluate the performance of restoration techniques for different image layouts.

The experimental results have shown that

(i) Assessed blur direction and blur length of blurred images are very close to theoretical value.

(ii) Lucy-Richardson based technique provides better result than Wiener based technique with the consideration of MSE, RMSE, NMAE and PSNR values for image layout .tif.

(iii) Lucy-Richardson based technique affords better result than Wiener based technique with the consideration of MSE, RMSE, and PSNR values for image layout .jpg whereas Wiener based technique provides better result in case of NMAE value.
(iv) Wiener based technique offers better result than Lucy-Richardson based technique with the consideration of MSE, RMSE, NMAE and PSNR values for image layout .png. Above performance results are shown for blurred images without noise.
(v) Fig. 4(a) displays input image which contains shadowing effect. Fig. 4(b) displays blur version of the input image and restored results illustrates that the shadowing effect spread over the whole image after reconstruct the blur image as shown in Fig. 4(c) and Fig. 4(d).

# References

[1] Haruka Asai, Yuji Oyamada, Julien Pilet, Hideo Satio, Cepstral analysis based blind deconvolution for motion blur, 17th IEEE International Conference on Image Processing., 978-1-4244-7993-1/10, Hong Kong, September, 2010.

[2] Michal Dobes, Libor Machala, Tomas Furst, Blurred Image Restoration: A fast method of finding the motion length and angle, Digital Signal Processing 20, 1677-1689, 1051-2004, 2010.

[3] Shamik Tiwari, V. P. Shukla, A. K. Singh and S. R. Biradar, Review of motion blur estimation techniques, Journal of Image and Graphics, Vol. 1, No. 4, December 2013.

[4] Joao P. A. Oliveira, Mario A. T. Figueiredo and Jose M. Bioucas-Dias, Blind estimation of motion blur parameters for image deconvolution, POSC/EEA-CPS/61271/2004.

[5] Hui Ji, Zuowei Shen and Yuhong Xu, Wavelet frame based image restoration with missing/degraded pixels, East Asia Journal on Applied Mathematics, 2011.

[6] Hongwei Sun, Michel Desvignes, Yunhui Yan, Weiwei Liu, Motion blur parameters identificationfrom radon tranform image gradient, IEEE IECON 978-1-4244-4649-0, December 2009.

[7] Wikky Fawwaz A M, Takuya Shimahashi, Mitsuru Matsubara and Sueo Sugimoto, PSF estimationand image restoration for noiseless motion blurres image, Proc. 7th IEEE WSEAS International Conference on Signal, Speech and Image Processing, Beijing, China, September 15-17, 2007.

[8] Rafael C. Gonzalez, Richard E. Woods, Digital Image Processing, Prentice Hall, 2007.

[9] Anil. K. Jain, Fundamental of Digital Image Processing, Prentice Hall, 1996.

[10] R.L.Lagendijk and J.Biemond. Hand Book of Image and Vedio Processing, chapter Basic Methods for Image Restoration and Identification, page 125-140.Academic Press, 2000.

[11] I.Rekleitis. Visual motion estimation based on motion blur interpretation. Masters thesis, School of Computer Science, McGill University, 1995.

[12] M.Cannon. Blind deconvolution of spatially invariant image blurs with phase, IEEE Trans. Acoust. Speech Signal Process., 24(1): 56-63, 1976.

[13] J. S. Lim. Image restoration by short space spectralsubtraction. IEEE Trans. Acoust. Speech SignalProcess., 28(2):191 197,1980.

[14] Deepa Kundur, Dimitrios Hatzinakos, A novel blind deconvolution scheme for image restoration using recursive filtering, IEEE Trans. on signal processing, Vol. 46, No. 2, February 1998.

[15] Reginald L. Lagendijk, Jan Biemond and Dick E. Boekee, Identification and restoration of noisy blurred images using the expectation-maximization algorithm, IEEE Trans. on acoustics, speech and signal processsing, VOL 38, NO. 7, July 1990.

[16] Alex Rav-Acha, Shmuel Peleg, Restoration of multiple images with motion blur in different directions, 5th IEEE Workshop on Applications of Computer Vision (WACV00), 0-7695-0813-8/00, 2000.

[17] Y. Yitzhaky, I. Mor, A. Lantzman and N. S. Kopeika, Direct method for restoration of motion-blurred images, Optical Society of America [S0740-3232(98)01406-9], 1998.

[18] Andreas Savakis, H. Joel Trussell, On the accuracy of PSF representation in image restoration, IEEE Trans. on image processing, Vol 2, No. 2, April 1993.

[19] Yuying Lu and Fadil Santosa, A computational algorithm for minimizing total variation in image restoration, IEEE Trans. on image processing, VOL 5, NO. 6, June 1996.

[20] R. Lokhande, K. V. Arya, and P. Gupta. 2006. Identification of parameters and restoration of motion blurred images. In Proceedings of the 2006 ACM symposium on Applied computing (SAC 06 ). ACM, New York, NY, USA, 301-305.

[21] R.Fergus, B. Singh, A. Hertzmann, S.T. Roweis, W.T. Freeman, Removing Camera Shake from a single photograph, In Proceedings of the 2006 ACM 0730-0301/06/0700-0787.